High-Performance and Highly Durable Inverted Organic Photovoltaics Embedding Solution-Processable Vanadium Oxides as an Interfacial Hole-Transporting Layer

Chih-Ping Chen, Yeu-Ding Chen, and Shih-Ching Chuang**

Energy sources and production are currently an important issues for human life. Renewable and green energy has been arguably the most accepted protocol for power generation in daily application. Solar energy technology, which uses abundant sources and is environmental friendly, is presently considered to be the developing technique. Thus, materials for efficient light-harvesting and power conversion play a significant role in such technology. Advanced materials, with characteristics of light weight, low temperature, large-area fabrication, inexpensiveness, and flexibility, have directed research toward thin-film technology, which is recognized as organic photovoltaics (OPVs).[1–12] The discovery of organic bulk heterojunction (OBHJ) thin-film technology with blended electron accepting and donating mixtures as an active layer had great impact on the field. In this technology, a normal cell (**Scheme 1**a) with the active layer consisting of a conjugated polymer, poly(3-hexylthiophene) (P3HT), and [6,6]-phenyl-C_{61} butyric acid methyl ester (PCBM)[13] as the key donor/acceptor pair embedded between electrodes of indium tin oxide (ITO)/poly(3,4-ethylenedioxythiophene):poly(styrenesulfonate) (PEDOT:PSS) and Ca/Al exhibits a promising power conversion efficiency (PCE). Improved PCEs of OBHJ technology through the innovation of p-type polymeric materials and cell engineering were also demonstrated.[14–17] Recently, Konarka and Solarmer have achieved record-high efficiency greater than 8%.[17,18] Despite its high efficiency, the stability of a normally configured photovoltaic device has been a primary concern for stepping into future marketing.[19] However, an inverted photovoltaic device (Scheme 1b), with metal oxides inserted between the active layer and ITO as the electron transporting layer (ETL) and PEDOT:PSS (PEDOT) embedded between active layer and metal electrodes (Ag) as hole transporting layer (HTL), exhibit much longer stability without much loss of efficiency.[20–23] The ubiquitous advantage of such cells highlights its tolerance to being built in the air. Although the inverted concept may provide a solution for the stability concerns, the tedious procedure for building up an inverted cell and the acidic nature of PEDOT cause another issues.[19] Therefore, research has been directed toward seeking functional interfacial materials that provide a facilitating procedure and enhanced performance.[24] The optimal materials require excellent ohmic contact with the active materials, good stability, and electron or hole blocking capability simultaneously. Attempts at engineering cheaper vanadium oxides (V_2O_5) for substituting PEDOT as an interlayer provided only limited success;[25] however, this was hampered by procedures including long annealing time (room temperature (rt), 3 d) using a suspension of V_2O_5 in isopropyl alcohol (IPA) and vacuum deposition.[21,26] In particular, it was noted that thinner layer (<10 nm) small island depositions, instead of uniform films, were formed; such a method made it less effective as a protection layer with vacuum-deposited V_2O_5. Our goal for establishing high-performance OPVs with long-term stability and easy hand-on and short-time fabrication procedures stimulates us to investigate solution-processable vanadium oxides (VO_x), via sol-gel processes, as an interlayer in inverted OPVs. The sol-gel VO_x-derived devices show durable PCE up to 5.0% under degradation test condition (65 °C, 1000 h); such OPVs also feature shorter annealing times than a suspension V_2O_5-derived device, which generally requires long-time annealing in the air (>48 h).

To render such sol-gel technique plausible for application in inverted OPVs, we first seek to understand the work function of the HTL material since it is a key parameter in determining device performance. In this study, a UV source was utilized to measure the ionization potential of materials in air using an AC2 photoelectron spectrometer. **Figure 1**a plots the square root of the counting rate (CR) as a function of the photon energy and the photoemission threshold energy. The work function or highest occupied molecular orbital (HOMO) level of the material was determined from the crossing point of the background and the yield line. The work function of PEDOT and the HOMO level of VO_x were determined to be –5.30 and –5.36 eV, respectively.[27–31] Figure 1b presents the resulting energy band diagram in relation to the relative energy levels of the acceptor (PCBM) used in this study and those of P3HT and alternating poly(thiophene-phenylene-thiophene)-(2,1,3-benzothiadiazole) (a-PTPTBT).[14] Since the work function of the VO_x is very close to that of PEDOT, the mismatch on energy levels of interface ingredients can be minimized using VO_x to substitute PEDOT as the HTL in OPVs. We also calculated the lowest unoccupied molecular orbital (LUMO) energy level of VO_x from edge of UV-vis spectrum (Figure 1a, inset). Notably, VO_x layer is advantageous on circumventing the electron transport and thereby the recombination nearby the anode.

Dr. C.-P. Chen, Y.-D. Chen
Materials and Chemical Laboratories
Industrial Technology Research Institute
Hsinchu, Taiwan, 31040, R.O.C
E-mail: chihping_chen@itri.org.tw
Prof. S.-C. Chuang
Department of Applied Chemistry
National Chiao Tung University
Hsinchu, Taiwan, 30010, R.O.C.
E-mail: jscchuang@faculty.nctu.edu.tw

DOI: 10.1002/adma.201102142

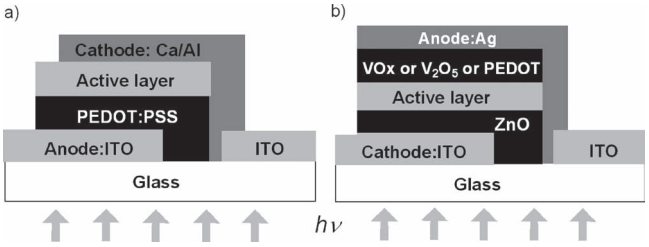

Scheme 1. Architecture of a normal (a) and an inverted (b) device.

To disclose the advances, we first delineate the general protocol for establishing highly stable and durable inverted cells. The inverted OPVs, with the layered configuration of glass/ITO/ZnO/polymer:PCBM/HTL/Ag, were fabricated using established methods.[32–35] We built up the active layer by spin-coating the blend solutions with various polymer-to-PCBM weight ratios in ortho-dichlorobenzene (*o*-DCB). The ETL of ZnO (50 nm) was deposited from a sol-gel process,[23] and for the hole-transporting VO_x layer, 0.05 M VTIPO solution (vanadium (V) triisopropoxy oxide) was spin-coated in the air under ambient conditions. The device was retained in the air for 10 min and then transferred to a glove box for thermal annealing at 100 °C for 5 min. The device was finalized by thermal deposition of 100 nm silver followed by encapsulation with UV-curing glue.

We used the above-developed protocol for establishing inverted cells embedding blending solution with P3HT:PCBM in the active layer and either with V_2O_5, VO_x or PEDOT as the HTL. **Table 1** lists the data of current density–voltage (*J*–*V*) characteristics of the studied devices and **Figure 2**a displays the *J*–*V* plots. The VO_x-derived devices show comparable levels of performance to those of suspension V_2O_5-derived and PEDOT-derived devices (entries 1–3). The previous approach with suspension of V_2O_5 material required long-time annealing in the air for 48 h (entry 1) and the PCE increases during this period. The reason for the necessity of long-time annealing with the suspension V_2O_5-derived device is not clear. The observed gradual development of PCE (≈0.5 to 3.8%) is primarily attributed to the change in interfacial behavior but not to morphology alteration of the active layer because the annealing procedures have been applied prior to HTL layer deposition. We infer that the observed gradual development of the PCE could be attributed to the oxidation of the silver contact. The Ag electrode in air can form an oxide layer that increases its effective work function from 4.3 to 5.0 eV and thereby enhances the device performance of the suspension V_2O_5-derived device.[36,37] We observed that the PCE was improved from 3.6% to 3.9% when a VO_x sol-gel is incorporated as the HTL (entry 2 and 3). The thickness of the VO_x layer controls the fill factor (FF) values. We observed that devices with a thinner VO_x layer, coated at 3000 rpm spinning rate to give optimal thickness of 25 nm, perform the best. The series resistance of the devices increased as the thickness of the VO_x layer went beyond the optimized one. The developed VO_x layer is also applicable to devices fabricated with another low bandgap conjugated polymer (a-PTPTBT),[14] as shown in Figure 1b. It is notable that the PCE was enhanced to 5.0% with combination of a-PTPTBT/VO_x as the polymer/HTL (entries 4 and 5), along with an open circuit voltage, V_{oc}, of 0.82 V, a short circuit current, J_{sc}, of 11.6 mA cm^{-2}, and a FF of 53.0%. We calculated the series resistance (R_s) and shunt resistance (R_{sh}) from the *J*–*V* curve. We observed a significant decrease in the R_s value upon using VO_x as the HTL with polymer a-PTPTBT from 28 to 7.7 Ω cm^{-2} (entries 4 and 5); however, such a dramatic decrease was not observed with PEDOT as the HTL (entries 2 and 3). The decrease in R_s implies that the bulk resistance of the devices becomes lower. Accordingly, a significant increase in R_{sh} from 266 to 390 Ω cm^{-2} is obtained (entry 4 versus 5). Such an outcome indicated that the interface defects caused charge recombination and the leakage current is lower for the VO_x device. Because the thinner active layer was used for the a-PTPTBT device (≈90 nm), the interfacial organization of VO_x at the junction contributed significantly to the performance enhancement.

Our interests in understanding the stability of devices prepared according to our new approaches led us to scrutinize their PCE degradation with time.[38–41] Thus, the degradation of encapsulated OPV devices under accelerated thermal annealing (65 °C) conditions in the air was investigated. Figure 2b shows the normalized PCEs as a function of time for respective devices. See Table S1 (Supporting Information) for degradation test of other normal and inverted cells. The normal cell (▼) with P3HT/PCBM shows a dissatisfying 50% decrease of the PCE at a time t = 250 h; however, the inverted cell (▲), composed of P3HT and PEDOT, remained at ≈85% of its initial efficiency value under accelerated thermal conditions for 1000 h. The limited lifetime is a result of several simultaneously complex processes. Known degradation mechanisms involve morphological changes,[42] degradation of the materials (active layer, electrode, and interfacial layer) by oxygen and water, interlayer and electrode diffusion, and electrode reaction with the organic materials.[19] By limiting the factors of oxygen and water, McGehee et al. have demonstrated a long lifetime normal cell device (poly[9′-hepta-decanyl-2,7-carbazole-alt-5,5-(4′,7′-di-2-thienyl-2′,1′,3′-benzothiadiazole) (PCDTBT)/[6,6]-phenyl-C_{71} butyric acid methyl ester ($PC_{71}BM$)) of up to 7 years, estimated by extrapolation based on state-of-the-art encapsulation.[43] As suggested by Fréchet et al., one can utilize materials engineering with crosslinkable materials to block the morphology development, and a stable normal cell was presented at high accelerated temperature (150 °C).[44,45] In another approach, Heeger et al. used interfacial engineering to improve the cell stability by insertion of titanium oxide (TiO_x) as a cathode interfacial layer and replacement of the PEDOT:PSS with molybdenum oxide (MoO_x).[46] The PCE of normal cells (ITO/MoO_x/PCDTBT/$PC_{71}BM$/TiO_x/Al) decay to approximately 50% of the original value after storage in air for 720 h and that of ITO/(PEDOT:PSS)/PCDTBT/$PC_{71}BM$/TiO_x/Al decay approximately 90% of the original value after storage in air for 480 h. Because the inverted cells often exhibit higher environmental stability,[20–23,47] the dissatisfying performance of our normal cell is most likely due to the low-work-function metal cathodes (Ca and Al).[48,49] It is known that Ca or Al electrodes can be easily oxidized using simple UV-glue encapsulation.[19]

According to previous procedure, an inverted device established with a V_2O_5 suspension in IPA as the HTL also displays a large drop in PCE, 45% and 40% of its initial values at t = 200 h and 1000 h, respectively (Figure 2b, ■). The eminent stability of devices built with a VO_x sol–gel process have been recorded

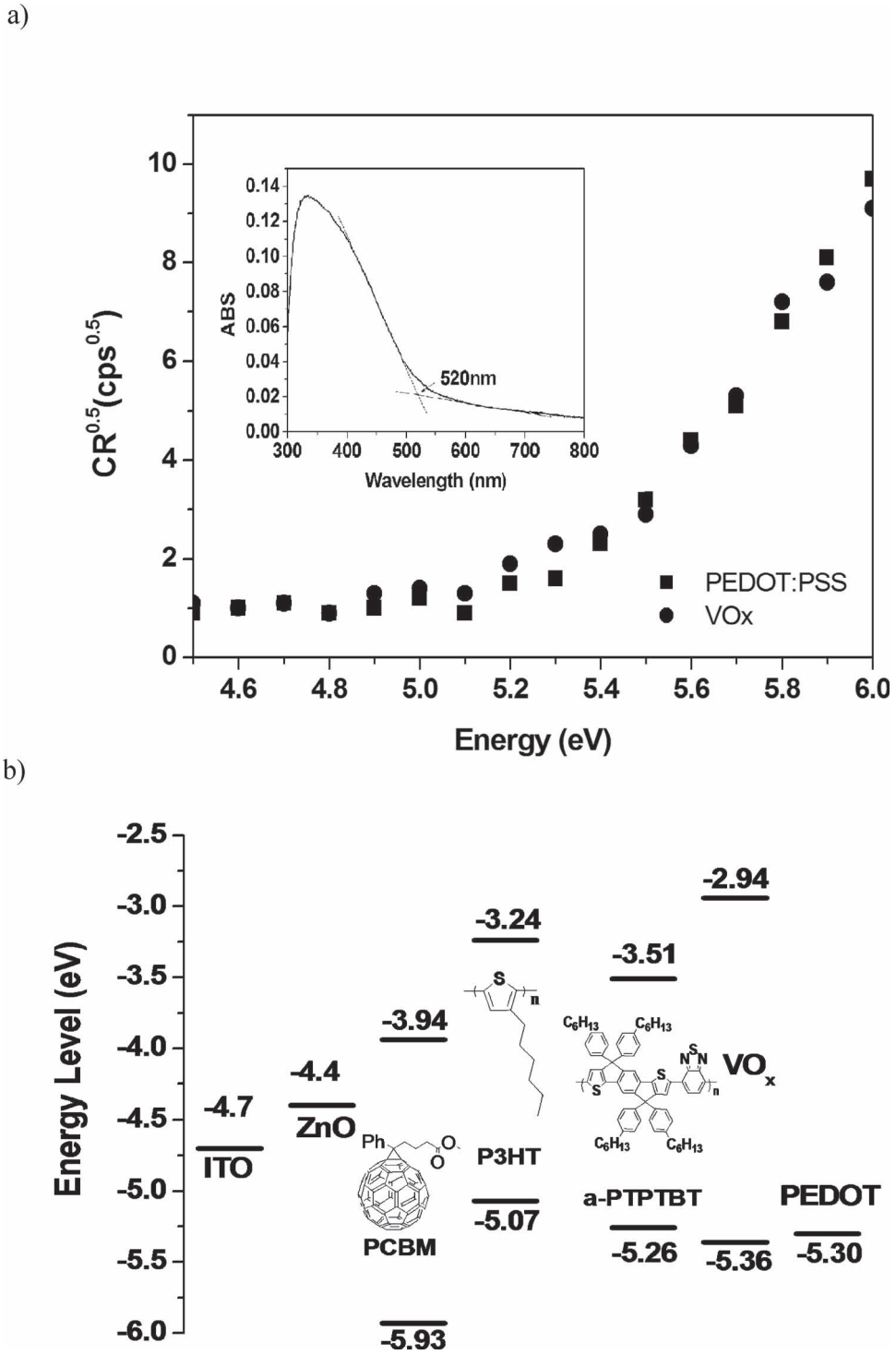

Figure 1. a) Photoelectron yield spectroscopy for PEDOT:PSS (■) and VO_x (●) films and UV-vis spectrum of VO_x (inset). b) Energy diagrams of respective materials.

without loss of PCE at $t = 1000$ h using either polymer P3HT (●) or a–PTPTBT (◆). The highly durable inverted OPVs built using our approaches feature obvious enhancement of thermal stability. The observed rough surface of the suspension-processed V_2O_5 (Figure S1a, Supporting Information) and the smooth structure obtained with VO_x sol–gel methods (Figure S1b, Supporting Information), recorded using scanning electron microscopy (SEM), rationalize their measured performance. This increase is attributed to the continuous feature of the solution-processed VO_x HTL, which forms a dense organic–inorganic

Table 1. OPV parameters of devices made with different polymer and HTL.

Entry	Polymer	HTL	J_{sc} [mA cm^{-2}]	V_{oc} [V]	FF	PCE [%]	R_s [Ω cm^{-2}]	R_{sh} [Ω cm^{-2}]
1[a)]	P3HT	V_2O_5	10.4	0.56	0.66	3.8	3.5	1226
2	P3HT	PEDOT	10.4	0.57	0.61	3.6	6.8	831
3	P3HT	VO_x	10.1	0.57	0.67	3.9	5.0	996
4	a-PTPTBT	PEDOT	9.7	0.82	0.45	3.6	28.0	266
5	a-PTPTBT	VO_x	11.6	0.82	0.53	5.0	7.7	390

[a)] The V_2O_5 was deposited according to methods in ref. [25].

hybrid layer, providing sufficient protection to the active layer while maintaining good device performance. The discontinued island distribution of suspension-processed V_2O_5 (Figure S1a, Supporting Information) caused interface instability through Ag diffusion into the polymer active layer during the long-term thermal annealing process. The PEDOT layer is potentially detrimental to the polymer active layer due to its acidic nature, which may dope the active layer and cause interface instability.

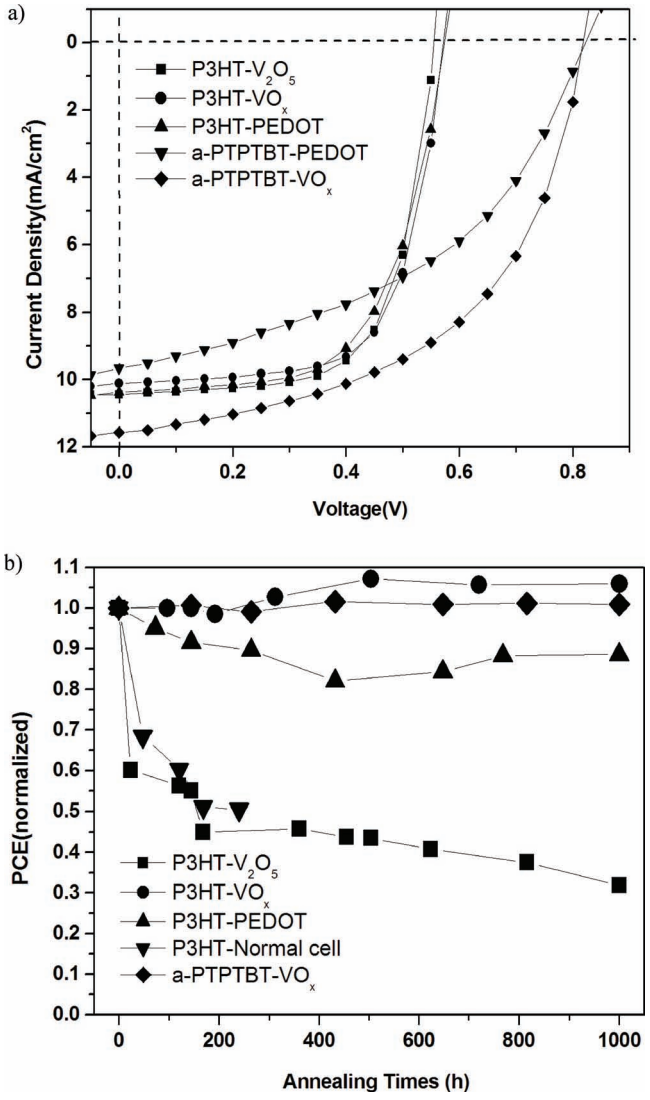

Figure 2. a) *J–V* curves of OPV devices with different active layers and hole transporting layers. b) Long-term thermal stability of the studied OPV devices.

In conclusion, we have presented an easy solution-processable method using VTIPO as the HTL for use in the inverted OPVs. The constructed devices show enhanced performance with the studied polymers through increasing the J_{sc} value and are highly durable throughout the investigated time periods. To the best of our knowledge, this is the first durability experiment that claims such long-term stability in the OPV with a high-performance, low-bandgap polymer. Further investigations of this developed vanadium oxides sol-gel technique on other new materials for high PCEs and durable devices for accelerated aging tests are currently underway.

Experimental Section

Photovoltaic Cell Fabrication and Testing: All bulk-heterojunction photovoltaic cells were prepared using the same preparation procedures and device fabrication procedure described below. The ITO substrates (obtained from Sanyo, Japan (8 Ω □$^{-1}$)) were first patterned by lithography, cleaned with detergent and ultrasonicated in acetone and isopropyl alcohol, dried on hot plate at 120 °C for 5 min, and finally treated with oxygen plasma for 5 min. The ZnO layer (50 nm) was spin-coated from a 0.5 M solution of zinc acetate in 2-methoxyethanol.[26] The P3HT devices were fabricated using a concentration of 15 mg mL^{-1} with a weight ratio of P3HT:$PC_{61}BM$ = 1:0.9 in chlorobenzene (CB) and a spin rate of 300 rpm for 60 s. The a-PTPTBT devices were fabricated using a-PTPTBT:$PC_{71}BM$ (weight ratio = 1:3) concentration of 10 mg mL^{-1} in *o*-DCB and a spin rate of 1200 rpm for 30 s. The P3HT devices were annealed at 150 °C for 10 min and the a-PTPTBT devices were solvent-annealed using saturated *o*-DCB vapor for 10 min. The optimal thickness of the P3HT- and a-PTPTBT-derived devices were 200 nm and 90 nm, respectively. PEDOT:PSS (Baytron P- VP AI4083) was filtered through a 0.45 μm filter before being deposited on an active layer with a thickness around 30 nm by spin coating at 3000 rpm in the air and drying at 100 °C for 10 min inside glove box. The VO_x layer was prepared from 0.05 M VTIPO (50 μL of vanadium (V) triisopropoxy oxide in 3.8 mL IPA and 0.2 mL deionized water mixture) solution and was spin-coated in air under ambient conditions. The device was aged in the air for 10 min and then transferred to glove box for thermal annealing at 100 °C for 5 min. The suspension V_2O_5-derived device was fabricated using the following procedure. The V_2O_5 powder was homogeneously dispersed and suspended in IPA at a concentration of 0.1 mg mL^{-1} using ultrasonic agitation.[25] The V_2O_5 suspension solution was then spin-casted on top of the photoactive layer at 3000 rpm in the air. Subsequently the devices were completed by depositing an 100 nm thick Ag layer under a pressure less than 10^{-6} Torr. The active area of the device was 5 mm^2.

It is worth noting that an extra annealing time (48 h) in air was utilized for suspension V_2O_5-derived device. Finally the cell was encapsulated using UV-curing glue (purchased from Nagase, Japan). During the encapsulation process, the UV-glue was dispensed onto the edge of a piece of glass in the air. The OPV device was covered with UV-glue-coated glass in the glove box. The device was then sealed by pressing the UV-glue coated glass on top of the device and the device underwent UV curing (254 nm) for 2 min. After encapsulation using UV-curing glue, we measured the *J–V* characteristics in air. *J–V* curves of the OPV devices were measured using a computer-controlled Keithley 2400 source measurement unit (SMU) equipped with a Peccell solar simulator under AM 1.5G illumination (100 mW cm^{-2}). The illumination intensity was calibrated using a standard Si photodiode detector equipped with a KG-5 filter. The output photocurrent was adjusted to match the photocurrent of the a Si reference cell for obtaining the power density of 100 mW cm^{-2}. After encapsulation, all device measurements were performed in an ambient atmosphere at 25 °C. The efficiency of 3.5% of a P3HT/PCBM reference cell measured under illumination in the laboratory was verified to be 3.4% under AM 1.5G conditions (100 mW cm^{-2}) at the National Institute of Advanced Industrial Science and Technology (AIST, Japan).

Supporting Information

Supporting Information is available from the Wiley Online Library or from the author.

Acknowledgements

The authors thank the Ministry of Economic Affairs and National Science Council (NSC962113M009028MY2) for financially supporting this research.

Received: June 8, 2011
Published online: July 22, 2011

[1] M. Helgesen, R. Søndergaard, F. C. Krebs, *J. Mater. Chem.* **2010**, *20*, 36.
[2] F. C. Krebs, S. A. Gevorgyan, J. Alstrup, *J. Mater. Chem.* **2009**, *19*, 5442.
[3] F. C. Krebs, *Sol. Energy Mater. Sol. Cell.* **2009**, *93*, 465.
[4] L. Blankenburg, K. Schultheis, H. Schache, S. Sensfuss, M. Schrödner, *Sol. Energy Mater. Sol. Cells.* **2009**, *93*, 476.
[5] P. Heremans, D. Cheyns, B. Rand, *Acc. Chem. Res.* **2009**, *42*, 1740.
[6] B. C. Thompson, J. M. J. Fréchet, *Angew. Chem. Int. Ed.* **2008**, *47*, 58.
[7] Y. He, Y. F. Li, *Phys. Chem. Chem. Phys.* **2011**, *13*, 1970.
[8] S. E. Shaheen, C. J. Brabec, N. J. Sariciftci, F. Padinger, T. Fromherz, J. C. Hummelen, *Appl. Phys. Lett.* **2001**, *78*, 841.
[9] C. J. Brabec, N. S. Sariciftci, J. C. Hummelen, *Adv. Funct. Mater.* **2001**, *11*, 15.
[10] M. M. Wienk, J. M. Kroon, W. J. H. Verhees, J. Knol, J. C. Hummelen, P. A. van Hal, R. A. J. Janssen, *Angew. Chem. Int. Ed.* **2003**, *42*, 3371.
[11] G. Li, V. Shrotriya, J. Huang, Y. Yao, T. Moriarty, K. Emery, Y. Yang, *Nat. Mater.* **2005**, *4*, 864.
[12] J. Y. Kim, K. Lee, N. E. Coates, D. Moses, T. -Q. Nguyen, M. Dante, A. J. Heeger, *Science* **2007**, *317*, 222.
[13] J. C. Hummelen, B. W. Knight, F. LePeq, F. Wudl, *J. Org. Chem.* **1995**, *60*, 532.
[14] Y.-C. Chen, C.-Y. Yu, Y.-L. Fan, L.-I. Hung, C.-P. Chen, C. Ting, *Chem. Commun.* **2010**, *46*, 6503.
[15] S. H. Park, A. Roy, S. Beaupré, S. Cho, N. Coates, J. S. Moon, D. Moses, M. Leclerc, K. Lee, A. J. Heeger, *Nat. Photonics* **2009**, *3*, 297.
[16] Y. J. He, H.-Y. Chen, J. H. Hou, Y. F. Li, *J. Am. Chem. Soc.* **2010**, *132*, 5532.
[17] H. Y. Chen, J. Hou, S. Zhang, Y. Liang, G. Yang, Y. Yang, L. Yu, Y. Wu, G. Li, *Nat. Photonics* **2009**, *3*, 649.
[18] R. F. Service, *Science* **2011**, *332*, 293.
[19] K. Norrman, M. V. Madsen, S. A. Gevorgyan, F. C. Krebs, *J. Am. Chem. Soc.* **2010**, *132*, 16883.
[20] L.-M. Chen, Z. Hong, G. Li, Y. Yang, *Adv. Mater.* **2009**, *21*, 1434.
[21] G. Li, C.-W. Chu, V. Shrotriya, J. Huang, Y. Yang, *Appl. Phys. Lett.* **2006**, *88*, 253503.
[22] Y. J. Cheng, C. H. Hsieh, Y. He, C.-S. Hsu, Y. F. Li, *J. Am. Chem. Soc.* **2010**, *132*, 17381.
[23] S. K. Hau, H.-L. Yip, N. S. Baek, J. Zou, K. O'Malley, A. K.-Y. Jen, *Appl. Phys. Lett.* **2008**, *92*, 253301.
[24] R. Po, C. Carbonera, A. Bernardi, N. Camaioni, *J. Mater. Chem.* **2011**, *4*, 285.
[25] J.-S. Huang, C.-Y. Chou, M.-Y. Liu, K.-H. Tsai, W.-H. Lin, C.-F. Lin, *Org. Electron.* **2009**, *10*, 1060.
[26] K. Takanezawa, K. Tjima, K. Hashimoto, *Appl. Phys. Lett.* **2008**, *93*, 063308.
[27] The VO_x layer was prepared from 0.05 M VTIPO (50 μL of vanadium (V) triisopropoxy oxide in 3.8 mL IPA and 0.2 mL deionized-water mixture) solution. The VO_x was then aged in the air for 10 min and then transferred to next process.
[28] B. B. Lakshmi, C. J. Patrissi, C. R. Martin, *Chem. Mater.* **1997**, *9*, 2544.
[29] D. P. Partlow, S. R. Gurkovich, K. C. Radford, L. J. Denes, *J. Appl. Phys.* **1991**, *70*, 443.
[30] T. T. Larsen-Olsen, E. Bundgaard, K. O. Sylvester-Hvid, F. C. Krebs, *Org. Electron.* **2011**, *12*, 364.
[31] N. Espinosa, H. F. Dam, D. M. Tanenbaum, J. W. Andreasen, M. Jørgensen, F. C. Krebs, *Materials* **2011**, *4*, 169.
[32] C.-P. Chen, S.-H. Chan, T.-C. Chao, C. Ting, B.-T. Ko, *J. Am. Chem. Soc.* **2008**, *130*, 12828.
[33] C.-Y. Yu, C.-P. Chen, S.-H. Chan, G.-W. Hwang, C. Ting, *Chem. Mater.* **2009**, *21*, 3262.
[34] S.-H. Chan, Y.-S. Hsiao, L.-I. Hung, G.-W. Hwang, H.-L. Chen, C. Ting, C.-P. Chen, *Macromolecules* **2010**, *43*, 3399.
[35] C.-P. Chen, C. Luo, C. Ting, S.-C. Chuang, *Chem. Commun.* **2011**, *47*, 1845.
[36] K.-H. Tsai, J.-S. Huang, M.-Y. Liu, C.-H. Chao, C.-Y. Lee, S.-C. Hung, C.-F. Lin, *J. Electrochem. Soc.* **2009**, *156*, B1188.
[37] M. S. White, D. C. Olson, S. E. Shaheen, N. Kopidakis, D. S. Ginley, *Appl. Phys. Lett.* **2006**, *89*, 143517.
[38] J. A. Hauch, P. Schilinsky, S. A. Choulis, S. Rajoelson, C. J. Brabec, *Appl. Phys. Lett.* **2008**, *93*, 103306.
[39] R. D. Bettignies, J. Leroy, M. Firon, C. Sentein, *Synth. Met.* **2006**, *156*, 510.
[40] J. A. Hauch, P. Schilinsky, S. A. Choulis, R. Childers, M. Biele, C. J. Brabec, *Sol. Energy Mater. Sol. Cells* **2008**, *92*, 727.
[41] B. Zimmermann, U. Würfel, M. Niggemann, *Sol. Energy Mater. Sol. Cells* **2009**, *93*, 491.
[42] A. Swinnen, I. Haeldermans, M. Ven, J. D'Haen, G. Vanhoyland, S. Aresu, M. D'Olieslaeger, J. Manca, *Adv. Funct. Mater.* **2006**, *16*, 760.
[43] C. H. Peters, I. T. Sachs-Quitana, J. P. Kastrop, S. Beaupré, M. Leclerc, M. D. McGehee, *Adv. Energy Mater.* DOI:10.1002/aenm.201100138.
[44] B. J. Kim, Y. Miyamoto, B. Ma, J. M. Fréchet, *Adv. Funct. Mater.* **2009**, *19*, 1.
[45] G. Griffini, J. D. Douglas, C. Piliego, T. W. Holcombe, S. Turri, J. M. J. Fréchet, J. L. Mynar, *Adv. Mater.* **2011**, *23*, 1660.
[46] Y. Sun, C. J. Takacs, S. R. Cowan, J. H. Seo, X. Gong, A. Roy, A. J. Heeger, *Adv. Mater.* **2011**, *23*, 2226.
[47] R. Po, C. Carbonera, A. Bernardi, N. Camaioni, *Energy Environ. Sci.* **2011**, *4*, 285.
[48] M. Jørgensen, K. Norrman, F. C. Krebs, *Sol. Energy Mater. Sol. Cells* **2008**, *92*, 686.
[49] M.-Y Lin, C.-Y. Lee, S.-C. Shiu, I.-J. Wang, J.-Y. Sun, W.-H. Wu, Y. H. Lin, J.-S. Huang, C.-F. Lin, *Org. Electron.* **2010**, *11*, 1828.